Environmental Science & Technology

Article

Cite This: Environ. Sci. Technol. 2019, 53, 14339−14347

pubs.acs.org/est

Abundant NH_3 in China Enhances Atmospheric HONO Production by Promoting the Heterogeneous Reaction of SO_2 with NO_2

Shuangshuang Ge,[†] Gehui Wang,*[,†,‡,§] Si Zhang,[†] Dapeng Li,[†] Yuning Xie,[†] Can Wu,[†] Qi Yuan,[∥] Jianmin Chen,[‡,⊥] and Hongliang Zhang[⊥]

[†]Key Lab of Geographic Information Science of the Ministry of Education, School of Geographic Sciences, East China Normal University, Shanghai 200241, China

[‡]Institute of Eco-Chongming, 3663 N. Zhongshan Road, Shanghai 200062, China

[§]CAS Center for Excellence in Regional Atmospheric Environment, Institute of Urban Environment, Chinese Academy of Sciences, Xiamen 361021, China

[∥]School of Earth Science, Zhejiang University, Hangzhou 310027, China

[⊥]Department of Environmental Science and Engineering, Fudan University, Shanghai 200043, China

Supporting Information

ABSTRACT: High levels of HONO have frequently been observed in Chinese haze periods and underestimated by current models due to some unknown sources and formation mechanisms. Combining lab-chamber simulations and field measurements in Xi'an and Beijing, China, we found that NH_3 can significantly promote HONO formation via the reduction−oxidation of SO_2 with NO_2 in the aqueous phase of hygroscopic particles (e.g., NaCl). Concentrations of HONO formed in the aerosol phase showed an exponential increase (R^2 = 0.91) with NH_3 levels under the chamber conditions and a linear growth with NH_3 levels in the two Chinese cities. The uptake coefficient of NO_2 on NaCl particles ranged from 2.0×10^{-5} to 1.7×10^{-4}, 3−4 orders of magnitude larger than that on water droplets. Our results further showed that HONO formed from the aerosol phase accounted for 4−33% of the total in the chamber, indicating that aerosol-phase formation is an important source of HONO in China, especially in haze periods. Since NH_3, SO_2, and NO_2 abundantly coexist in China, the positive effect of NH_3 on HONO formation could enhance the atmospheric oxidizing capacity in the country, causing severe secondary aerosol pollution. Our work suggests that NH_3 emission control is imperative for mitigating air pollution in China.

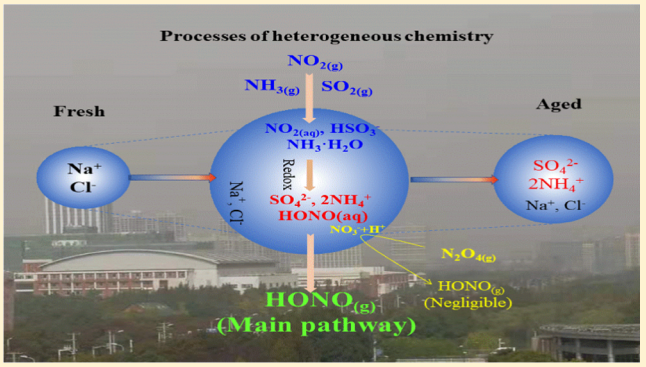

1. INTRODUCTION

Nitrous acid (HONO) is the major precursor of hydroxyl (OH) radicals.[1−3] Studies have revealed that the photolysis of HONO (R1) contributes up to 60% of the integrated OH radical budget in the daytime and serves as a major source of OH radicals in the first 2−3 hours after sunrise.[4−8]

$$\mathrm{HONO} + h\nu(\lambda \leq 390\ \mathrm{nm}) \rightarrow \mathrm{NO} + {}^{\bullet}\mathrm{OH} \qquad \text{(R1)}$$

Since the OH radical is the primary oxidant in the atmosphere and drives the chemistry of ozone production and OH-initiated secondary aerosol formation,[3,7,9,10] HONO plays a crucial role in the atmospheric chemistry of the lower troposphere.

Heterogeneous conversion of NO_2 on different surfaces is believed to be the dominant mechanism of HONO formation.[3,11−13] A previous work has indicated that the asymmetric dissociation of NO_2 dimers (N_2O_4) on the air−water interface of clouds, fog droplets, and wet aerosols, along with the reduction−oxidation reaction of NO_2 monomers on soot surfaces, is likely the major secondary formation process of HONO in the lower troposphere.[2,10,11,14,15] In addition, based on theoretical calculations, Li et al.[16] proposed that in a water droplet system, NH_3 may enhance HONO formation by promoting the disproportional hydrolysis of N_2O_4. This formation is enabled because NH_3 could markedly reduce the free-energy barrier of hydrolysis of N_2O_4 into HONO and HNO_3. However, the applicability and importance of the above-proposed mechanisms for the dissociation of N_2O_4 in the real atmosphere are still controversial. For example, Colussi et al.[17] reported that the ratio of $[N_2O_4]/[NO_2]$ is less than 10^{-5} when the concentration of NO_2 is 1 ppm, which means that the N_2O_4 concentration in a typical urban atmospheric environment is very low (<1 ppt) and can be ignored, even

Received: August 8, 2019
Revised: November 8, 2019
Accepted: November 11, 2019
Published: November 11, 2019

DOI: 10.1021/acs.est.9b04196
Environ. Sci. Technol. 2019, 53, 14339−14347

under heavily polluted conditions (e.g., NO_2 = 100 ppb); these conclusions suggest that the formation pathway of HONO via the asymmetric dissociation of N_2O_4 in the atmosphere is probably not as important as previously thought.

In addition to the above dissociation formation pathway, the possibility of HONO formation via the reduction−oxidation of NO_2 with SO_2 in the aerosol aqueous phase has been investigated very recently. For example, a laboratory work showed that NO_2 could be almost entirely dissociated into HONO and HNO_3 within a very short time (<50 μs) on the gas−liquid interface of $NaHSO_3$ droplets, with no reaction with the S(IV) anion.[3] However, combing atmospheric measurements in Chinese megacities and laboratory experiments, Wang et al.[2] proposed that gaseous HONO can be efficiently produced via the heterogeneous oxidation of SO_2 by NO_2 in wet aerosols with NH_3 neutralization, especially in the severe haze periods of China. Laboratory denuder experiments have shown that mixed gases of NO_2 and SO_2 can produce more HONO than NO_2 in purified air, indicating the promoting role of SO_2 in HONO formation.[18] Ma et al.[19] also reported that the reductive effect of SO_2 can increase the heterogeneous conversion of NO_2 to HONO on the surface of MgO. These different results suggest that an investigation of the formation mechanism of NO_2 into HONO involving S(IV) and NH_3 in the atmosphere is warranted.

Due to the tremendous demand for nitrogen fertilizers and livestock in China, the levels of atmospheric NH_3 in the country are very high both in rural and urban areas and are 1 order of magnitude higher than those in the US and Europe.[20] Meanwhile, SO_2 and NO_x emissions in China are also severe due to the large amount of combustion of fossil fuels in the country. NH_3, NO_2, SO_2, and aerosol particles coexist abundantly in the urban atmosphere of China and undergo fast multiphase reactions under humid conditions, which have not only caused severe haze pollution but also resulted in a high level of HONO throughout the country, especially during the winter.[2] Nevertheless, the source and formation mechanism of HONO in China is still unclear.

In the current work, we quantitatively investigated the effect of NH_3 on HONO formation under humid conditions, in the absence and presence of hygroscopic seeds, by using a smog chamber, along with field investigations on the relationship of the winter nighttime HONO and NH_3 in two Chinese megacities. To the best of our knowledge, this is the first time that the effect of NH_3 on HONO formation from the aerosol phase has been quantified. Our work revealed that aerosol aqueous-phase formation is an important source of HONO in the polluted atmosphere of China.

2. EXPERIMENTAL SECTION

2.1. Laboratory Smog Chamber Simulation. *2.1.1. Materials and Methods.* A homemade smog chamber, with dimensions of 1.1 m × 0.8 m × 1.2 m, which is comprised of an outer layer of a 5.6 mm-thick acrylic shell and an inner layer of a 0.13 mm Teflon bag, was used in this study. The experimental details have been provided in our previous work;[2,21] here, we only give a brief description as follows.

To investigate the HONO formation on the chamber surface and the wet aerosols, simulation experiments with and without seed particles were conducted in this work, respectively. A background gas of zero air was produced by the Zero Air Supply (model 111 and model 1150, Thermo Scientific). Many studies have found that the rapid formation of severe haze in China often occurred under very humid conditions with a relative humidity (RH) larger than 90%,[2,22] and thus a 90% RH condition was applied in this work to investigate the mechanism of HONO formation in haze periods of China. A flow of humid vapor that was generated by bubbling zero air through ultrapure water (Milli Q, 18.2 MΩ, Millipore Ltd.) was introduced into the chamber to obtain the designed RH. The reaction temperature was maintained at 298 K (room temperature). For the experiments with seed particles, a single jet atomizer (7388SJA, TSI) was used to generate seed aerosols. NaCl particles with 100 nm diameter were introduced into the chamber after being dried by two tandem Nafion dryers and selected by a differential mobility analyzer. The initial concentration of the NaCl seeds was approximately 1×10^4 cm^{-3}. The reaction gases of SO_2, NO_2, and NH_3, which were purchased from Air Liquide Holding Co., Ltd. (China), were injected sequentially into the reactor chamber directly with a syringe.

2.1.2. Chamber Online Monitoring and Particle Analysis. HONO formed during the experiments was measured by a long-path absorption photometer (LOPAP-03, QUMA, Germany), while reactant gases of NO, NO_2, and SO_2 in the chamber were measured by Thermo Scientific analyzers (NO_x and SO_2 analyzers). The size distribution and mass concentrations of particles in the chamber were measured by a scanning mobility particle sizer (SMPS). Chemical compositions of the particles in the chamber were measured by using transmission electron microscopy (TEM), coupled with energy-dispersive X-ray spectrometry (EDX),[23] and ion chromatography (IC), respectively. The schematic depiction of the injection and measurement system of the chamber experiments is shown in Figure S1. More details about the measurements above can be found in the Supporting Information.

All of the chamber experiments were conducted under dark conditions by fully covering the chamber with an anti-UV cloth hood. Prior to each experiment, the chamber was flushed with zero air for at least 15 h to ensure that the particles inside the chamber were undetectable for the SMPS instrument. The static electricity on the surface of the chamber was removed by using two ironing air blowers around the chamber.

2.1.3. Smog Chamber Experiments. To investigate the influences of water vapor and background gases on HONO formation, experiments with different background gases (99.9995% N_2, 99.9995% synthetic air, or zero air), under dry (0% RH) and high-humidity (~90% RH) conditions, were conducted using the 1 m^3 chamber. Influences of different concentrations of NH_3 (0.05−2.0 ppm) on HONO formation were investigated under the two RH conditions. All experiments were conducted at 1 atm and room temperature (298 K). The initial conditions of the experiments are listed in Table S1.

2.2. Field Measurements in Two Chinese Megacities. Field measurements of gaseous and aerosol pollutants were performed in Beijing and Xi'an, China, respectively. From 15th Dec. 2017 to 25th Feb. 2018, a field campaign was conducted on the rooftop of a two-story building at the Institute of Atmospheric Physics of the Chinese Academy of Sciences (CAS), which is located in Beijing, near the 4th-ring freeway. The Xi'an campaign was performed from 17th Nov. to 12th Dec. 2012. The observation site was located on the rooftop of a three-story building on the campus of the Institute of Earth Environment, CAS. During the two field campaigns, inorganic

DOI: 10.1021/acs.est.9b04196
Environ. Sci. Technol. 2019, 53, 14339−14347

ions of $PM_{2.5}$ and gaseous pollutants including HONO, SO_2, and NH_3 were monitored using an In situ Gas and Aerosol Compositions Monitor (IGAC, Fortelice International Co., Taiwan), with a time resolution of 1 h. The details of the instrumentations and methods can be found elsewhere.[2,24,25]

3. RESULTS AND DISCUSSION

3.1. Effects of NH_3 on HONO Formation in the Absence of Seed Particles. In the experiments under dry conditions (0% RH) without seeds or any other artificially introduced particulate matter, pure nitrogen gas was chosen to serve as the background gas. No HONO was formed after introducing NO_2 into the reactor under the dry conditions, even when NH_3 and SO_2 were further introduced into the chamber. These results showed that the surface liquid water is indispensable for HONO formation. Moreover, acidic and/or alkaline gases do not have any influence on HONO formation in the absence of surface water during the experimental period.

In the experiments under 90% RH conditions without seed particles, a level of 21 ± 3 ppb HONO was detected, which was formed via the hydrolysis reaction of NO_2 (0.6 ppm) on the inside surface of the chamber (Figure 1a, phase I). As shown in Figure 1a, in phase II, the subsequent introduction of 1 ppm NH_3 into the chamber after the equilibrium of NO_2 hydrolysis did not cause any changes to the HONO level, which suggests that NH_3 cannot promote the conversion of NO_2 to HONO. However, as seen in Figure 1a, in phase III, we observed a 2-fold increase in the HONO level (increased by about 38 ppb on average) when the reductive gas (SO_2, 0.6 ppm) was introduced into the chamber, suggesting that there is a synergetic effect of SO_2, NO_2, and NH_3 on HONO formation under the high-humidity conditions, in which the HONO formation is much more efficient than the hydrolysis of NO_2 alone.

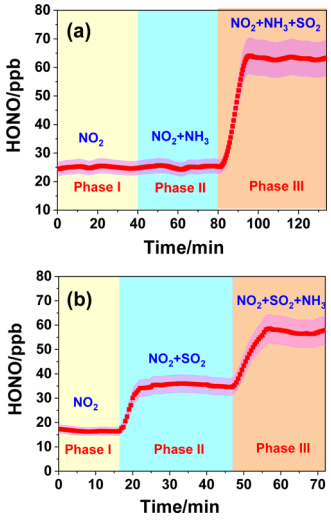

Figure 1. Variation of HONO concentration as a function of reaction time under 90% RH conditions without seeded aerosols (initial concentrations of NO_2, SO_2, and NH_3 in the chamber were 0.6, 0.6, and 1.0 ppm, respectively).

To further identify the roles of NH_3 and SO_2 in the HONO formation process, parallel experiments that introduced SO_2 and NH_3 into the chamber were conducted. Figure 1b shows the HONO level variation after introducing NO_2, NH_3, and SO_2 with an order different from that in Figure 1a. As seen in Figure 1b, the HONO level increased by approximately 1-fold from 17 ppb in phase I to 35 ppb in phase II after introducing 0.6 ppm SO_2, and then further increased by approximately 1-fold from 35 to 57 ppb in phase III after introducing NH_3, which increased by a total of ~40 ppb on average (Figure 1b, phase III), suggesting that the reductive SO_2 alone can promote the conversion of NO_2 to HONO, but the degree of conversion is lower than that with the synergistic effect of SO_2 and NH_3 together. These parallel experiments revealed that NH_3 can enhance the partitioning of SO_2 into the wet chamber surface and then promote the formation of HONO via the reduction−oxidation reaction of NO_2 with SO_2.[2,26] Therefore, NH_3 can promote HONO formation indirectly. Since NO_2, NH_3, and SO_2 levels are high in China, especially during winter haze periods, the role of NH_3 in promoting HONO formation in the atmosphere is expected to be significant.

Based on the molecular dynamics simulation, Li et al.[16] proposed that HONO can be readily formed from the NH_3-promoted hydrolysis of the NO_2 dimer (N_2O_4) by reducing the energy barrier to HONO formation at room temperature. Some laboratory studies have also pointed out that N_2O_4 is an intermediate in the conversion of NO_2 to HONO.[11,27] However, the concentration of N_2O_4 under real atmospheric conditions is extremely low (6×10^{-5} ppb, which is approximately several orders of magnitude lower than that of NO_2), suggesting that the formation pathway of HONO via the dissociation of N_2O_4 in the real atmosphere is not as significant as previously thought.[12] This is the reason why in the above chamber simulations, we did not observe an enhancing effect of NH_3 on HONO formation in the absence of SO_2, since the concentration of NO_2 that we used for the chamber simulation is close to that in a typical urban atmosphere. Based on this work, we believe that the role of NH_3 in promoting HONO formation in the real atmosphere results from an increase in the partitioning of SO_2 into the aqueous phase and a subsequent promotion of the reduction−oxidation reaction of NO_2 with SO_2. Furthermore, the formation of HONO is not due to the enhanced dissociation of N_2O_4 because its concentration is too low in the real atmosphere.

3.2. Influence of NH_3 on HONO Formation in the Real Atmosphere and in the Chamber Study. The field observations from Beijing, China, in winter from 15th Dec. 2017 to 25th Feb. 2018 showed that the average concentration of NH_3 increased from 6 ppb in the clean periods ($PM_{2.5}$ < 35 $\mu g\ m^{-3}$) to greater than 18 ppb in the polluted periods ($PM_{2.5}$ > 75 $\mu g\ m^{-3}$).[25] Due to the rapid photolysis of HONO in the daytime, in this study, we only focused on the impact of NH_3 on HONO at night (from 18:00 p.m. to 6:00 a.m.). Due to the strict emission controls and favorable meteorological conditions (lower RH and high wind speed), air pollution in Beijing during the 2017 winter was much more mitigated. For example, on average, $PM_{2.5}$ was only 39.7 $\mu g\ m^{-3}$ during the campaign with HONO levels being less than 3 ppb. As seen in Figure 2a, the nighttime HONO in Beijing during the campaign showed a good linear correlation with $NH_3(g)$ (R^2 = 0.57). Xi'an is located in Guanzhong Basin in inland China, where a periodic cycle of 4−5 days of pollution episodes has frequently occurred in winter.[2] Our field observation in Xi'an, China, from 17th Nov. to 12th Dec., 2012, showed that the concentration of NH_3 increased from 6 ± 3 ppb on clean days to 14 ± 7 ppb on polluted days with a daily maximum of more than 60 ppb. As seen in Figure 2b, the nighttime

DOI: 10.1021/acs.est.9b04196
Environ. Sci. Technol. 2019, 53, 14339−14347

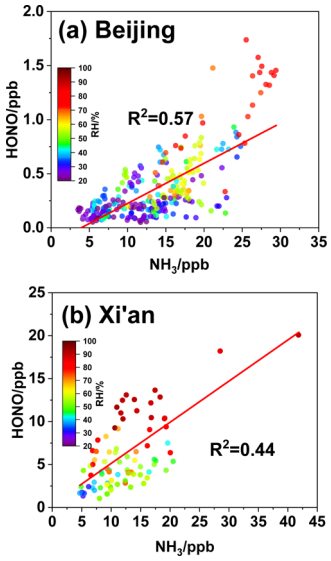

Figure 2. Linear fit regression for nighttime NH_3 and HONO(g) in two Chinese megacities: (a) Beijing from 15th Dec. 2017 to 25th Feb. 2018 and (b) Xi'an from 17th Nov. to 2nd Dec. 2012.

concentrations of HONO also showed a clear linear correlation with NH_3 (R^2 = 0.44) (Figure 2b). The positive correlation between NH_3 and HONO in the two cities indicates a possible mechanism between NH_3 and HONO that leads to a promoting effect of NH_3 on HONO formation in the real atmosphere. According to the results of Wang et al.,[2] the measured HONO concentration during the polluted days was inversely correlated to SO_2, which suggests that its formation mechanism is related to the aqueous oxidation of SO_2 by NO_2.

To understand the reaction process under the severe haze conditions of China and the quantitative effect of NH_3 on the heterogeneous formation of HONO, we investigated the variations in the concentration of HONO as a function of NH_3 concentration in a $NO_2/SO_2/NH_3$/NaCl system, by using the smog chamber simulation. As shown in Figure 3, the

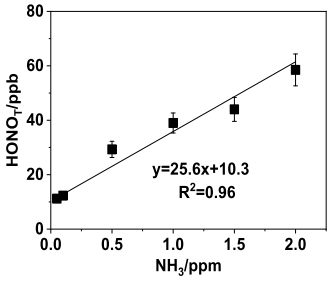

Figure 3. Relationship between total formed $HONO_T$ and NH_3 in the $NO_2/SO_2/NH_3$/NaCl system ($HONO_T$ is the total concentration of HONO formed in the chamber with the presence of NH_3 and SO_2 under 90% RH conditions).

concentration of HONO formed in the chamber ($HONO_T$) linearly increased with the increasing NH_3 levels (R^2 = 0.96), ranging from 11 to 57 ppb when the introduced NH_3 increased from 0.05 to 2.0 ppm. The measured HONO was the total concentration of HONO ($HONO_T$) formed from the chamber surface ($HONO_C$) and the aerosol aqueous phase ($HONO_A$), as the surface effect of the chamber in the laboratory experiment cannot be eliminated. Although the realistic atmosphere is borderless, buildings, plants, and soil can provide surfaces that influence the formation of HONO. Thus, our chamber study is still representative of the real atmosphere (large surface-to-volume ratio).

To further clarify the mechanism of HONO formation, chemical compositions of the products formed on the seeded particles were analyzed using transmission electron microscopy (TEM), coupled with energy-dispersive X-ray spectrometry (EDX), and ion chromatography (IC) (Figure 4). The EDX images in Figure 4a–d show that except for the peaks from the substrate itself (C, O, and Si) and NaCl from the seed itself (Figure 4b), the signals of N and S emerged, and the O signal increased in the products at the end of the experiments (Figure 4d). The much lower IC signal intensities of N than those of S in the particles collected after the reactions clearly suggest that the dissolved NO_2 was hardly converted to NO_3^-, while SO_2 was transformed to sulfate in the aerosol phase (Figure 4d). The IC results also showed that the mass concentration of NO_3^- was 1 order of magnitude lower than that of sulfate (Figure 4e and Table S2), again demonstrating that the heterogeneous formation of HONO did not proceed via the N_2O_4 dissociation pathway but via the pathway of SO_2 oxidation by NO_2 with a product of sulfate. Because all of the experiments were conducted without solar irradiation, the photolysis of HONO could not proceed, which is consistent with the fact that no nitric oxide (NO) was formed over the experimental period in the chamber. Therefore, the possibility of SO_2 oxidation by an OH radical that was produced from HONO decomposition can be completely ruled out, and sulfate in the chamber was produced solely from the reduction–oxidation of SO_2 with NO_2.

In this work, the pH values of the particles formed in the chamber were estimated using the ISORROPIA-II thermodynamic model, which was 5.3 ± 0.2 under the 2.0 ppm NH_3 conditions and 4.6 ± 0.1 under the 0.05 ppm NH_3 conditions, respectively, which is consistent with the results reported by Cheng et al.,[28] who used the WRF-CMAQ model to simulate the winter haze formation in China and found that under the humid conditions of Chinese haze periods, the oxidation of SO_2 by NO_2 started to play a more important role in sulfate formation at an aerosol pH of ∼5.0.

3.3. Heterogeneous Formation of HONO in the Aqueous Phase of Atmospheric Aerosols. Previous works have revealed that HONO in the lower atmosphere is mainly formed on different wet surfaces,[10,11,29] and a larger surface-to-volume ratio (S/V) is favorable for HONO formation.[11] Several lab studies have indicated that aerosol particles are possible contributors to HONO production in the urban atmosphere during severe haze periods.[2,8,19,27] However, until now, there has been no investigation on the importance of this process. Here, we quantify the relative contribution of HONO formed in the aerosol phase compared to that in the atmosphere, based on our laboratory smog chamber experiment.

As mentioned above, the amount of HONO formed in the aerosol phase cannot be directly measured, as it mixes with the HONO gas released from the chamber surface. Thus, we used the amount of sulfate formed in the seed particles to calculate the concentration of HONO formed on the NaCl seed particles, based on the following stoichiometry:[2]

$$SO_2(g) + 2NO_2(g) + 2NH_3(g) + 2H_2O(aq) \rightarrow 2NH_4^+(aq) + SO_4^{2-}(aq) + 2HONO(g) \quad (R2)$$

DOI: 10.1021/acs.est.9b04196
Environ. Sci. Technol. 2019, 53, 14339–14347

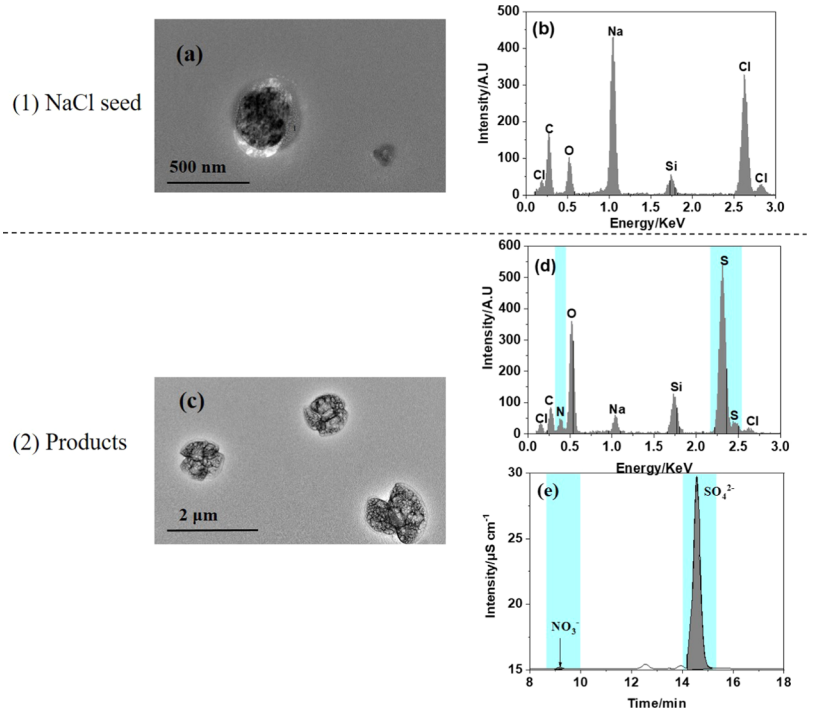

Figure 4. Morphology and compositions of seeded NaCl particles in the chamber before and after exposure to $NO_2/SO_2/NH_3$ gases: TEM (a) and EDX (b) images of the seeded particles before the exposure; TEM (c) and EDX (d) images of the seeded particles after the exposure for 1 h; and (e) ion chromatogram of seeded NaCl particles collected after 1 h of the exposure.

Table 1. HONO Formation and Particle Growth during the Experiments in the $NO_2/SO_2/NH_3$/NaCl System (90% RH; T = 25 °C)[a]

NH_3/ppm	0.05	0.1	0.5	1.0	1.5	2.0
GF, Dp_t/D_0	1.04	1.11	1.16	1.27	1.42	1.89
$(NH_4)_2SO_4/\mu g\ m^{-3}$	1.3	4.0	6.3	11.6	20.3	51.8
$HONO_T$/ppb	11.2	12.3	29.3	39.0	44.0	56.6
$HONO_A$/ppb	0.5	1.5	2.3	4.2	7.4	18.9

[a]Note: GF, growth factor of particles (Dp_t/D_0); $HONO_T$, total concentration of HONO formed in the chamber; $HONO_A$, concentration of HONO formed in the aerosol aqueous phase.

The diameter of particles increased with higher NH_3 in the $NO_2/SO_2/NH_3$/seed system (Figure S2). We assumed that all of the particles were spherical, and the size growth of NaCl aerosols is the result of the coating of ammonium sulfate. Therefore, the formed ammonium sulfate can be determined based on the growth factor (GF) of particles, which is defined as the ratio of the dry particle diameter (Dp_t) at the time t of the experiment to that (Dp_0) at the beginning of the experiment, as shown by Equation 1 (eq E1). Then, the formed HONO on the aerosol particles ($HONO_A$) can be calculated by using Equation 2 (eq E2):

$$GF = \frac{D_{P_t}}{D_{P_0}} \quad \text{(E1)}$$

$$[HONO_A] = 2 \times \frac{(GF^3 - 1) \times [NaCl]_0}{M_{(AS)}} \times \frac{T}{T_0} \times V_m \quad \text{(E2)}$$

where $HONO_A$ is the concentration (ppb) of HONO formed on the aqueous aerosol, $[NaCl]_0$ is the initial concentration ($\mu g\ m^{-3}$) of NaCl seed particles, T and T_0 are the temperatures (298 and 273 K, respectively), $M_{(AS)}$ is the formula mass of ammonium sulfate (AS, g mol^{-1}), and V_m is the molar volume of the gas at 1 atm (L mol^{-1}). The amounts of sulfate and HONO formed in the aerosol aqueous phase are listed in Table 1.

With the increase of NH_3 concentrations, the formed HONO produced on the chamber surface and the aerosol particles increased. However, the amount of HONO formed on the chamber surface tended to become saturated under high-NH_3 conditions (Figure 5a). In contrast, an exponential growth of HONO formed in the aerosol bulk solution with an increasing NH_3 level was observed (Figure 5b). The main reason for the exponential increase of HONO under higher-NH_3 conditions was the synergistic effects of NH_3 and aerosol particles (Figure 5c,d). The presence of NH_3 showed multiple effects over the course of the experiments. NH_3 can promote the dissolution of SO_2 into the aerosol aqueous phase as HSO_3^- and SO_3^{2-}, both of which were subsequently oxidized by NO_2 into ammonium sulfate and HONO(g) via the reduction−oxidation reactions. The formed ammonium sulfate can not only increase the mass of aerosols but can also absorb water vapor, leading to an increase in the surface area and aqueous phase volume of the aerosols, which can in turn further promote the heterogeneous reaction of the dissolved NO_2, NH_3, and SO_2[2,19] (Figure 6).

DOI: 10.1021/acs.est.9b04196
Environ. Sci. Technol. 2019, 53, 14339−14347

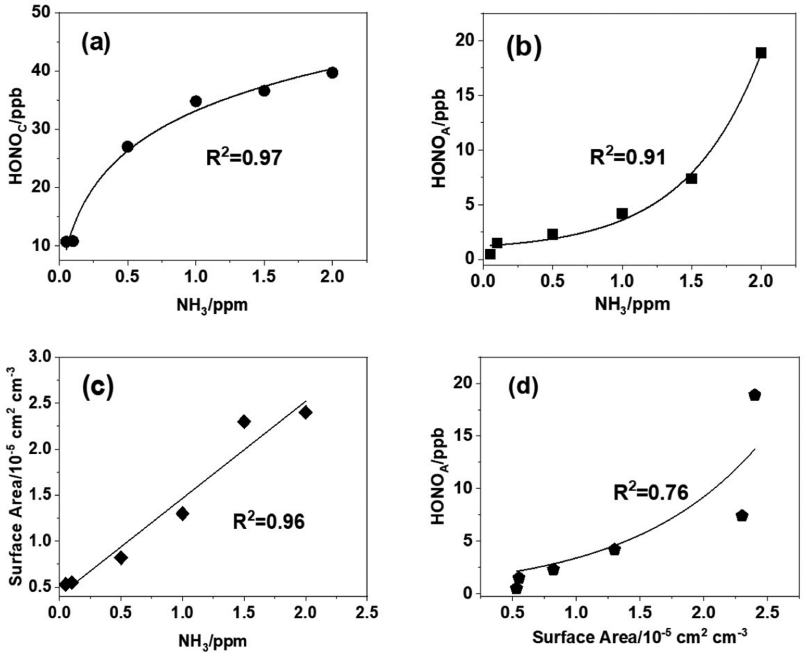

Figure 5. Variation of HONO concentration with increasing NH_3 levels in the chamber: (a) concentration of HONO formed on the chamber surface (HONOc); (b) concentration of HONO formed in the aerosol bulk solution ($HONO_A$); (c) surface area of particles as a function of NH_3 concentration; and (d) concentration of HONO formed in the aerosol solution as a function of the surface area of the particles in the chamber.

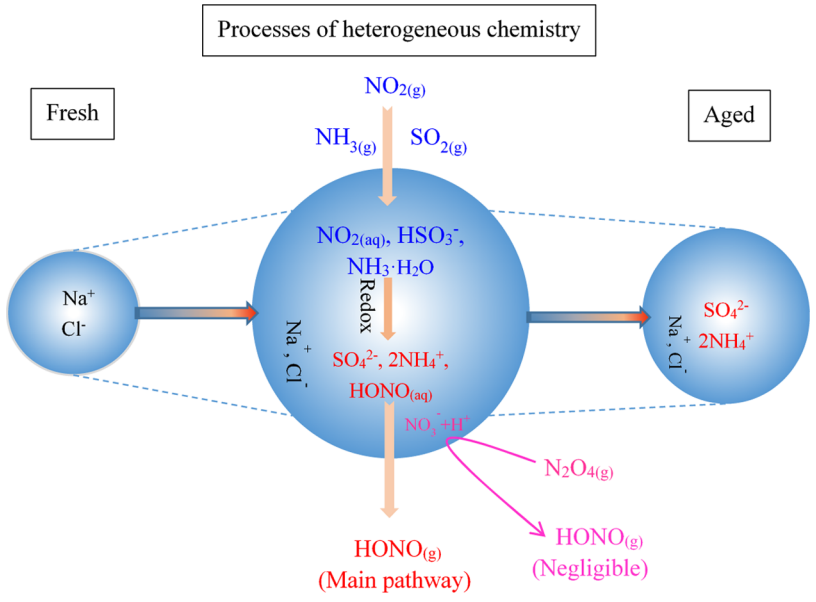

Figure 6. Schematic plot of the HONO formation mechanism in the urban atmosphere of China during haze events.

Based on our chamber simulation, we proposed two formation pathways for HONO gas in the urban atmosphere; one is wet-surface asymmetric dissociation without SO_2 and the other is the aerosol bulk-phase reduction−oxidation with SO_2.

In the absence of SO_2,

$$2NO_2(g) + H_2O(aq) \rightarrow HONO(aq) + HNO_3(aq) \quad (R3)$$

$$HONO(aq) \rightarrow HONO(g) \quad (R4)$$

In the presence of SO_2,

$$NO_2(g) \rightarrow NO_2(aq) \quad (R5)$$

$$SO_2(g) + NH_3(g) + H_2O(aq) \rightarrow HSO_3^-(aq) + NH_4^+(aq) \quad (R6)$$

$$2NO_2(aq) + HSO_3^-(aq) + H_2O(aq) \rightarrow 2HONO(aq) + SO_4^{2-}(aq) + H^+(aq) \quad (R7)$$

$$HONO(aq) \rightarrow HONO(g) \quad (R8)$$

The overall reaction of NO_2 with SO_2 in the aerosol aqueous phase is as follows:

DOI: 10.1021/acs.est.9b04196
Environ. Sci. Technol. 2019, 53, 14339−14347

$$2NO_2(aq) + HSO_3^-(aq) + NH_3(aq) + H_2O \rightarrow 2HONO(aq) + SO_4^{2-}(aq) + NH_4^+(aq) \quad (R9)$$

$$HONO(aq) \rightarrow HONO(g) \quad (R10)$$

The surface area ($0.5-2.4 \times 10^{-3}$ m^2 m^{-3}) of the dry aerosol particles in our chamber was 3−4 orders of magnitude lower than that of the Teflon reactor (6 m^2 m^{-3}). However, the $HONO_A$ formed on the aerosol aqueous phase was in the range of 0.5−19 ppb when NH_3 increased from 0.05 to 2.0 ppm, which accounted for approximately 4−33% of the total $HONO_T$ in the chamber. HONO(g) in the urban atmosphere is believed to be mainly produced from different surfaces including urban building surfaces, soil, and vegetation.[11,30,31] To evaluate the importance of the aerosol-phase production of HONO relative to the urban surfaces, we transformed the production rate of $HONO_A$ in the aerosol bulk solution into the aerosol surface and compared it with the HONO formed on the inside surface of the chamber, based on the stoichiometry of R9. As shown in Table S3, we found that the HONO production rate per unit surface area of aerosol particles was $9.4-79 \times 10^4$ ppb m^{-2} m^3, which was approximately 4−5 orders of magnitude higher than that on the chamber wall surface, suggesting that the aerosol-phase production of HONO is important in the atmosphere. Due to its large specific surface area, the equilibrium of HONO vapor pressure over an aerosol aqueous phase can be reached much faster than that over the liquid surface of a bulk solution. Thus, the HONO (aq) formed from the aerosol phase in the chamber was rapidly released into the gas phase as HONO(g) (R10), which in turn promoted reaction R9.

A previous work suggested that the dissociated product (NO_2^-) of HONO in the aqueous phase can react with HSO_3^-, forming SO_4^{2-} and HSO_4^-.[32] To investigate the potential impact of NO_2^- oxidation on the sulfate production in the chamber, we calculated the possible contribution of sulfate derived from NO_2^- oxidation to the total sulfate aerosols, based on the reaction rate parameters given by Oblath et al.[32,33] As shown in Table S4, under the 0.05 and 2.0 ppm NH_3(g) conditions, the levels of aerosol-phase NO_2^- in the chamber were 0.07 and 1.20 μg m^{-3}, respectively, which are about 2 orders of magnitude lower than that in the gas phase ($HONO_T$), suggesting that HONO formed via the oxidation of SO_2 by NO_2 mostly stays in the gas phase. Under such chamber conditions, the maximum concentrations of SO_4^{2-} derived from the NO_2^- oxidation with S(IV) were 0.06 and 0.39 μg m^{-3} at the two NH_3 levels, respectively (Table S4), which are less than 6 percent of the total sulfate aerosols in the chamber, suggesting that the sulfate production due to the reaction of NO_2^- with HSO_3^- in this work was minor and the sulfate in the chamber was almost entirely derived from the SO_2 oxidation by NO_2.

To further evaluate the efficiency of the aerosol-phase HONO production, we calculated the uptake coefficient of NO_2 on the seeded NaCl particles. HONO formation via the uptake of NO_2 is parameterized as a first order loss of NO_2.[3] The mass balance and stoichiometry of HONO formation can be described as follows:

$$\frac{d[HONO]}{dt} = \frac{1}{4} \times \gamma \bar{C} \left(\frac{S}{V}\right)[NO_2(g)] \quad (E3)$$

where [HONO] is the mass concentration (μg m^{-3}) of HONO produced during a time period t, γ is the uptake coefficient, $\bar{C}$ is the mean molecular speed (cm s^{-1}), S/V is the aerosol surface area (cm^2 cm^{-3}), and [NO_2(g)] is the NO_2 concentration (μg m^{-3}) in the gas phase. Based on Equation 3 (eq E3), the mean value of γ was calculated to be in the range of $2.0 \times 10^{-5}-1.7 \times 10^{-4}$. This result is consistent with previous work, which showed that NO_2(g) uptake coefficients on sea-salt aerosols were 3−4 orders of magnitude higher than those on water ($10^{-8}-10^{-7}$) and could reach up to 10^{-4}.[34,35]

During severe haze periods in China, the amount of $PM_{2.5}$ can reach up to hundreds of micrograms per cubic meter.[2,21] Typical S/V values of aerosols in Beijing during haze periods are $\sim 5 \times 10^{-5}$ cm^2 cm^{-3}, and on the level of 2×10^{-5} cm^2 cm^{-3} even in clean periods,[26,36] which is comparable to the seeded aerosol surface area under our chamber experimental conditions ($0.5-2.4 \times 10^{-5}$ cm^2 cm^{-3}). Therefore, the efficient formation of HONO in the aerosol phase observed in this work is representative of the real atmospheric conditions and suggests that the aerosol-phase reduction−oxidation of SO_2 with NO_2, with a neutralization effect of NH_3, is an important source of HONO in China during haze periods.

4. IMPLICATIONS FOR ATMOSPHERIC CHEMISTRY

The total NH_3 emissions in China have increased from 12.1 ± 0.8 Tg N yr^{-1} in 2000 to 15.6 ± 0.9 Tg N yr^{-1} in 2015 with an annual increase rate of 1.9% and account for approximately 20% of the total NH_3 emissions in the world,[37,38] among which nitrogen fertilizers are the dominant sources. However, vehicle emissions, coal burning, and power plants are also important sources of NH_3, especially in the urban areas of China.[39] High NH_3 emissions from both agricultural and nonagricultural sources have resulted in much heavier NH_3 pollution than those in developed countries. For example, Meng et al.[20] reported a daily NH_3(g) concentration of 350 ppb with an hourly maximum of 800 ppb during the summer of 2013 at Gucheng, a rural site in North China Plain (NCP). Due to the abundant alkaline NH_3 gas, atmospheric aerosols in China are moderately acidic with a pH higher than 4 (even 6),[28] which is much higher than that (~2) in the US[40] and favorable for the efficient formation of sulfate during the haze periods in China.[2,28]

This work demonstrates that NH_3 can enhance the atmospheric oxidation capacity by accelerating the aerosol-phase formation of HONO in the atmosphere. The high uptake coefficient ($10^{-5}-10^{-4}$) of NO_2 on hygroscopic NaCl particles under humid conditions indicates that the aerosol-phase production of HONO is comparable to that of the total urban ground surface in the haze periods of China, which can explain the high levels of HONO observed in Xi'an and Beijing, China.[2] Since HONO is labile and can optically decompose into an OH radical, the efficient aerosol-phase formation of HONO is likely one of the factors resulting in the high concentration of OH radicals in Beijing, even in severe haze events.[15,41] The abundant OH radicals further react with NO_2 and organic precursors, significantly enhancing the secondary aerosol contribution to particulate pollution in the country.[2,21] $PM_{2.5}$ levels in many cities of China have been decreasing significantly since 2013 because the Chinese government has taken several measures to reduce SO_2, NO_x, and smoke emissions from power plants and traffic exhausts. However, $PM_{2.5}$ levels in the country, especially in the North China Plain during winter, are still much higher than those in

DOI: 10.1021/acs.est.9b04196
Environ. Sci. Technol. 2019, 53, 14339−14347

developed countries and far beyond the World Health Organization standard. Our work suggests that emission controls on NH_3 gas are necessary for further mitigating $PM_{2.5}$ pollution in the country.

■ ASSOCIATED CONTENT

Supporting Information

The Supporting Information is available free of charge at https://pubs.acs.org/doi/10.1021/acs.est.9b04196.

Plot of the chamber system, size growth of NaCl particles with different NH_3 concentrations, initial conditions of the chamber simulations, chemical composition of particles in the chamber, comparison of HONO formed on the chamber surface and the aerosols, details of the chamber online monitoring and particle analysis, and calculations on HONO partitioning and sulfate formation by the oxidation of NO_2^- with HSO_3^- (PDF)

■ AUTHOR INFORMATION

Corresponding Author

*E-mail: ghwang@geo.ecnu.edu.cn. Tel: 86-21-54341193. Fax: 86-21-54341122.

ORCID

Shuangshuang Ge: 0000-0002-3797-6838

Hongliang Zhang: 0000-0002-1797-2311

Notes

The authors declare no competing financial interest.

■ ACKNOWLEDGMENTS

This work was financially supported by the National Natural Science Foundation of China (Nos 41773117 and 41807355), National Key R&D Plan programs (Nos 2017YFC0210005 and 2017YFC0212703), and the China Postdoctoral Science Foundation (No. 2018M632061).

■ REFERENCES

(1) Sörgel, M.; Regelin, E.; Bozem, H.; Diesch, J. M.; Drewnick, F.; Fischer, H.; Harder, H.; Held, A.; Hosaynali-Beygi, Z.; Martinez, M.; Zetzsch, C. Quantification of the unknown HONO daytime source and its relation to NO_2. *Atmos. Chem. Phys.* **2011**, *11*, 10433−10447.

(2) Wang, G.; Zhang, R.; Zamora, M. L.; Gomez, M. E.; Yang, L.; Hu, M.; Lin, Y.; Guo, S.; Meng, J.; Li, J.; Cheng, C.; Hu, T.; Ren, Y.; Wang, Y.; Gao, J.; Cao, J.; An, Z.; Zhou, W.; Wang, J.; Marrero-Ortiz, W.; Tian, P.; Secrest, J.; Peng, J.; Du, Z.; Zheng, J.; Shang, D.; Zeng, L.; Shao, M.; Wang, W.; Huang, Y.; Wang, Y.; Zhu, Y.; Li, Y.; Hu, J.; Pan, B.; Cai, L.; Cheng, Y.; Rosenfeld, D.; Liss, P. S.; Duce, R. A.; Kolb, C. E.; Molina, M. J. Persistent sulfate formation from London fog to Chinese haze. *Proc. Natl. Acad. Sci. U.S.A.* **2016**, *113*, 13630−13635.

(3) Li, L. J.; Hoffmann, M. R.; Colussi, A. J. The role of nitrogen dioxide in the production of sulfate during Chinese haze-aerosol episodes. *Environ. Sci. Technol.* **2018**, *52*, 2686−2693.

(4) Czader, B. H.; Rappenglück, B.; Percell, P.; Byun, D. W.; Ngan, F.; Kim, S. Modeling nitrous acid and its impact on ozone and hydroxyl radical during the Texas Air Quality Study 2006. *Atmos. Chem. Phys.* **2012**, *12*, 6939−6951.

(5) Alicke, B.; Platt, U.; Stutz, J. Impact of nitrous acid photolysis on the total hydroxyl radical budget during the limitation of oxidant production/pianura padana produzione di ozono study in Milan. *J. Geophys. Res.* **2002**, *107*, No. 8196.

(6) Vogel, B.; Vogel, H.; Kleffmann, J.; Kurtenbach, R. Measured and simulated vertical profiles of nitrous acid - Part II. Model simulations and indications for a photolytic source. *Atmos. Environ.* **2003**, *37*, 2957−2966.

(7) Kleffmann, J.; Gavriloaiei, T.; Hofzumahaus, A.; Holland, F.; Koppmann, R.; Rupp, L.; Schlosser, E.; Siese, M.; Wahner, A. Daytime formation of nitrous acid: A major source of OH radicals in a forest. *Geophys. Res. Lett.* **2005**, *32*, No. L05818.

(8) Fu, X.; Wang, T.; Zhang, L.; Li, Q.; Wang, Z.; Xia, M.; Yun, H.; Wang, W.; Yu, C.; Yue, D.; Zhou, Y.; Zheng, J.; Han, R. The significant contribution of HONO to secondary pollutants during a severe winter pollution event in southern China. *Atmos. Chem. Phys.* **2019**, *19*, 1−14.

(9) Ge, S.; Xu, Y.; Jia, L. Secondary organic aerosol formation from propylene irradiations in a chamber study. *Atmos. Environ.* **2017**, *157*, 146−155.

(10) Xu, W.; Ye, K.; Zhao, C.; Tao, J.; Zhao, G.; Bian, Y.; Yu, Y.; Shen, C.; Liang, L.; Zhang, G. NH_3-promoted hydrolysis of NO_2 induces explosive growth in HONO. *Atmos. Chem. Phys.* **2019**, *19*, 10557−10570.

(11) Finlayson-Pitts, B. J.; Wingen, L. M.; Sumner, A. L.; Syomin, D.; Ramazan, K. A. The heterogeneous hydrolysis of NO_2 in laboratory systems and in outdoor and indoor atmospheres: An integrated mechanism. *Phys. Chem. Chem. Phys.* **2003**, *5*, 223−242.

(12) Gustafsson, R. J.; Kyriakou, G.; Lambert, R. M. The molecular mechanism of tropospheric nitrous acid production on mineral dust surfaces. *Chem. Phys. Chem.* **2008**, *9*, 1390−1393.

(13) Kinugawa, T.; Enami, S.; Yabushita, A.; Kawasaki, M.; Hoffmann, M. R.; Colussi, A. J. Conversion of gaseous nitrogen dioxide to nitrate and nitrite on aqueous surfactants. *Phys. Chem. Chem. Phys.* **2011**, *13*, 5144−5149.

(14) Hou, S.; Tong, S.; Ge, M.; An, J. Comparison of atmospheric nitrous acid during severe haze and clean periods in Beijing, China. *Atmos. Environ.* **2016**, *124*, 199−206.

(15) Liu, Z.; Wang, Y.; Costabile, F.; Amoroso, A.; Zhao, C.; Huey, L. G.; Stickel, R.; Liao, J.; Zhu, T. Evidence of aerosols as a media for rapid daytime HONO production over China. *Environ. Sci. Technol.* **2014**, *48*, 14386−14391.

(16) Li, L.; Duan, Z. Y.; Li, H.; Zhu, C. Q.; Henkelman, G.; Francisco, J. S.; Zeng, X. C. Formation of HONO from the NH_3-promoted hydrolysis of NO_2 dimers in the atmosphere. *Proc. Natl. Acad. Sci. U.S.A.* **2018**, *115*, 7236−7241.

(17) Colussi, A. J.; Enami, S.; Yabushita, A.; Hoffmann, M. R.; Liu, W. G.; Mishra, H.; Goddard, W. A. Tropospheric aerosol as a reactive intermediate. *Faraday Discuss.* **2013**, *165*, 407−420.

(18) Spindler, G.; Hesper, J.; Brüggemann, E.; Dubois, R.; Müller, Th.; Herrmann, H. Wet annular denuder measurements of nitrous acid: laboratory study of the artefact reaction of NO_2 with S(IV) in aqueous solution and comparison with field measurements. *Atmos. Environ.* **2003**, *37*, 2643−2662.

(19) Ma, Q.; Wang, T.; Liu, C.; He, H.; Wang, Z.; Wang, W.; Liang, Y. SO_2 initiates the efficient conversion of NO_2 to HONO on MgO surface. *Environ. Sci. Technol.* **2017**, *51*, 3767−3775.

(20) Meng, Z.; Xu, X.; Lin, W.; Ge, B.; Xie, Y.; Song, B.; Jia, S.; Zhang, R.; Peng, W.; Wang, Y.; Cheng, H.; Yang, W.; Zhao, H. Role of ambient ammonia in particulate ammonium formation at a rural site in the North China Plain. *Atmos. Chem. Phys.* **2018**, *18*, 167−184.

(21) Wang, G.; Zhang, F.; Peng, J.; Duan, L.; Ji, Y.; Marrero-Ortiz, W.; Wang, J.; Li, J.; Wu, C.; Cao, C.; Wang, Y.; Zheng, J.; Secrest, J.; Li, Y.; Wang, Y.; Li, H.; Li, N.; Zhang, R. Particle acidity and sulfate production during severe haze events in china cannot be reliably inferred by assuming a mixture of inorganic salts. *Atmos. Chem. Phys.* **2018**, *18*, 10123−10132.

(22) Wu, L. Y.; Sun, J. Y.; Zhang, X. Y.; Zhang, Y. M.; Wang, Y. Q.; Zhong, J. T.; Yang, Y. Aqueous-phase reactions occurred in the PM2.5 cumulative explosive growth during the heavy pollution episode (HPE) in 2016 Beijing wintertime. *Tellus B* **2019**, *71*, 11−15.

(23) Li, W.; Shao, L.; Zhang, D.; Ro, C.; Hu, M.; Bi, X.; Geng, H.; Matsuki, A.; Niu, H.; Chen, J. A review of single aerosol particle studies in the atmosphere of East Asia: morphology, mixing state,

DOI: 10.1021/acs.est.9b04196
Environ. Sci. Technol. 2019, 53, 14339−14347

source, and heterogeneous reactions. *J. Clean. Prod.* **2016**, *112*, 1330−1349.
(24) Wang, G. H.; Cheng, C. L.; Huang, Y.; Tao, J.; Ren, Y. Q.; Wu, F.; Meng, J. J.; Li, J. J.; Cheng, Y. T.; Cao, J. J.; Liu, S. X.; Zhang, T.; Zhang, R.; Chen, Y. B. Evolution of aerosol chemistry in Xi'an, inland China, during the dust storm period of 2013, Part 1: Sources, chemical forms and formation mechanisms of nitrate and sulfate. *Atmos. Chem. Phys.* **2014**, *14*, 11571−11585.
(25) Xie, Y.; Wang, G.; Wang, X.; Chen, J.; Chen, Y.; Tang, G.; Wang, L.; Ge, S.; Xue, G.; Wang, Y.; Gao, J. Observation of nitrate dominant $PM_{2.5}$ and particle pH elevation in urban Beijing during the winter of 2017. *Atmos. Chem. Phys. Discuss.* **2019**, No. 541.
(26) Liu, J.; Fang, S.; Liu, W.; Wang, M.; Tao, F. M.; Liu, J. Y. Mechanism of the Gaseous hydrolysis reaction of SO_2: Effects of NH_3 versus H_2O. *J. Phys. Chem. A* **2015**, *119*, 102−111.
(27) Liu, C.; Ma, Q.; Liu, Y.; Ma, J.; He, H. Synergistic reaction between SO_2 and NO_2 on mineral oxides: A potential formation pathway of sulfate aerosol. *Phys. Chem. Chem. Phys.* **2012**, *14*, 1668−1676.
(28) Cheng, Y.; Zheng, G.; Wei, C.; Mu, Q.; Zheng, B.; Wang, Z.; Gao, M.; Zhang, Q.; He, K.; Carmichael, G.; Pöschl, U.; Su, H. Reactive nitrogen chemistry in aerosol water as a source of sulfate during haze events in China. *Sci. Adv.* **2016**, *2*, No. e1601530.
(29) Arens, F.; Gutzwiller, L.; Baltensperger, U.; Gäggeler, H.; Ammann, M. Heterogeneous reaction of NO_2 on diesel soot particles. *Environ. Sci. Technol.* **2001**, *35*, 2191−2199.
(30) Su, H.; Cheng, Y. F.; Oswald, R.; Behrendt, T.; Trebs, I.; Meixner, F. X.; Andreae, M. O.; Cheng, P.; Zhang, Y.; Poschl, U. Soil nitrite as a source of atmospheric HONO and OH radicals. *Science* **2011**, *333*, 1616−1618.
(31) Stutz, J.; Alicke, B.; Neftel, A. Nitrous acid formation in the urban atmosphere: Gradient measurements of NO_2 and HONO over grass in Milan, Italy. *J. Geophys. Res. Atmos.* **2002**, *107*, No. 8192.
(32) Oblath, S. B.; Markowitz, S. S.; Novakov, T.; Chang, S. G. Kinetics of the formation of hydroxylamine disulfonate by reaction of nitrite with sulfites. *J. Phys. Chem. A* **1981**, *85*, 1017−1021.
(33) Oblath, S. B.; Markowitz, S. S.; Novakov, T.; Chang, S. G. Kinetics of the initial reaction of nitrite ion in bisulfite solutions. *J. Phys. Chem. A* **1982**, *86*, 4853−4857.
(34) Yabushita, A.; Enami, S.; Sakamoto, Y.; Kawasaki, M.; Hoffmann, M. R.; Colussi, A. J. Anion-catalyzed dissolution of NO_2 on aqueous microdroplets. *J. Phys. Chem. A.* **2009**, *113*, 4844−4848.
(35) Abbatt, J. P. D.; Waschewsky, G. C. G. Heterogeneous interactions of HOBr, HNO_3, O_3, and NO_2 with deliquescent NaCl aerosols at room temperature. *J. Phys. Chem. A* **1998**, *102*, 3719−3725.
(36) Kinugawa, T.; Enami, S.; Yabushita, A.; Kawasaki, M.; Hoffmann, M. R.; Colussi, A. J. Conversion of gaseous nitrogen dioxide to nitrate and nitrite on aqueous surfactants. *Phys. Chem. Chem. Phys.* **2011**, *13*, 5144−5149.
(37) Zhang, Xi.; Wu, Y.; Liu, X.; Reis, S.; Jin, J.; Dragosits, U.; Van Damme, M.; Clarisse, L.; Whitburn, S.; Coheur, P.; Gu, B. Ammonia emissions may be substantially underestimated in China. *Environ. Sci. Technol.* **2017**, *51*, 12089−12096.
(38) Gu, B.; Ju, X.; Chang, J.; Ge, Y.; Vitousek, P. M. Integrated reactive nitrogen budgets and future trends in China. *Proc. Natl. Acad. Sci. U.S.A.* **2015**, *112*, 8792−8797.
(39) Qiu, C.; Zhang, R. Multiphase chemistry of atmospheric amines. *Phys. Chem. Chem. Phys.* **2013**, *15*, 5738−5752.
(40) Weber, R. J.; Guo, H.; Russell, A. G.; Nenes, A. High aerosol acidity despite declining atmospheric sulfate concentrations over the past 15 years. *Nat. Geosci.* **2016**, *9*, 282−286.
(41) Tang, Y.; An, J.; Wang, F.; Li, Y.; Qu, Y.; Chen, Y.; Lin, J. Impacts of an unknown daytime HONO source on the mixing ratio and budget of HONO, and hydroxyl, hydroperoxyl, and organic peroxy radicals, in the coastal regions of China. *Atmos. Chem. Phys.* **2015**, *15*, 9381−9398.

DOI: 10.1021/acs.est.9b04196
Environ. Sci. Technol. 2019, 53, 14339−14347